



Accepted Article

Title: Synthesis of Nonstoichiometric $\text{Cu}_2\text{ZnSnS}_4$ by cation exchange of ZnS

Authors: Yi Jin and George Chumanov

This manuscript has been accepted after peer review and appears as an Accepted Article online prior to editing, proofing, and formal publication of the final Version of Record (VoR). This work is currently citable by using the Digital Object Identifier (DOI) given below. The VoR will be published online in Early View as soon as possible and may be different to this Accepted Article as a result of editing. Readers should obtain the VoR from the journal website shown below when it is published to ensure accuracy of information. The authors are responsible for the content of this Accepted Article.

To be cited as: *Eur. J. Inorg. Chem.* 10.1002/ejic.201700137

Link to VoR: <http://dx.doi.org/10.1002/ejic.201700137>

Synthesis of Nonstoichiometric $\text{Cu}_2\text{ZnSnS}_4$ by cation exchange of ZnS

Yi Jin, George Chumanov*

Corresponding Authors: *E-mail: gchumak@clemson.edu

<http://www.clemson.edu/science/departments/chemistry/people/faculty/chumanov.html>

Department of Chemistry, Center for Optical Materials Science and Engineering Technologies (COMSET), Clemson University, Clemson, South Carolina 29634, United States

Key words: $\text{Cu}_2\text{ZnSnS}_4$, Zn-rich, solar cells, Raman spectrum, nanocrystals

Abstract

A cation exchange reaction of wide band gap crystalline ZnS with CuCl_2 and SnCl_4 in triethylene glycol was developed to synthesize nonstoichiometric $\text{Cu}_2\text{ZnSnS}_4$ with crystallite size more than 100 nm. The materials were characterized by powder X-ray diffraction, electron microscopy, Raman, and energy dispersive X-ray elemental mapping. The method allows the formation of Zn-rich phases and good control of the crystal size and shape. No narrow bandgap high conductive Cu_xS impurities were observed.

Introduction

$\text{Cu}_2\text{ZnSnS}_4$ (CZTS) is a p-type semiconductor with a band gap of 1.4–1.6 eV and a high light absorption coefficient of over 10^4 cm^{-1} .^[1] It is made of earth-abundant and nontoxic elements and has good stability in the ambient environment. CZTS is investigated as a light absorption material in solar cells,^[2] photocatalyst^[3] and photocathode for water splitting^[1,4]. A range of techniques is used to synthesize CZTS, including organic solvent assistant direct synthesis,^[4] hydro/solvent thermal synthesis, chemical vapor deposition,

pulse laser deposition, sputtering, evaporation, electrochemical deposition, sol-gel coating, spray pyrolysis, and successive ionic layer absorption and reaction.^[1] Sulfurization by H₂S or S at around 500 °C is an essential step in all these methods to obtain highly crystallized CZTS. The high-temperature sulfurization of CZTS also results in sulfurization of metal oxide semiconductors such as ZnO, TiO₂, thereby limiting *in situ* fabrication of highly efficient solar cells. As synthesized, CZTS is also often contaminated with impurities such as highly conductive or narrow bandgap Cu_xS, Sn_xS, and Cu-Sn-S.^[5] These impurities trap carriers and act as recombination centers. As a result, electrons and holes cannot reach the surface of the semiconductor leading to low conversion efficiency of photocatalysts and low open circuit voltage, current density and fill factor in solar cells.

Polycrystalline and amorphous materials have also much more crystal defects and dangling bonds than single crystal materials and these disorder states increase the carrier scattering thereby decreasing their lifetime, mobility, and diffusion length. The semiconductor in the single crystal state shows significantly better carrier mobility and diffusion length than in the polycrystalline and amorphous states. However, there is no effective method currently available for low temperature synthesis of large crystals of pure CZTS. Furthermore, many studies have shown that Zn-rich CZTS exhibits much better photovoltaic effect than Cu-rich CZTS.^[2] Therefore, it is essential to develop an effective method for the synthesis of highly crystalline CZTS with the full control of Zn concentration in the product. Cation exchange reactions is an effective method to synthesize complex compounds with certain morphologies.^[6] The first cation exchange synthesis of CZTS was the reaction of Cu₂SnS₃ with zinc diethyldithiocarbamate in a mixture of 1-dodecanethiol and trioctylamine at 250 °C resulting in ~15 nm CZTS

nanoparticles.^[7] However, the synthesis of large crystals of the reactant Cu_2SnS_3 was shown to be difficult. CZTS thin plates with a thickness of about 12 nm were also synthesized by the cation exchange of CuS with zinc 2,4-pentanedionate monohydrate and tin(IV)chloride bis(2,4-pentanedionate) in a mixture of oleylamine, sulfur and 1-dodecanethiol at 260 °C.^[8] In a slightly modified method, in which CuS with $\text{Zn}(\text{CH}_3\text{COO})_2 \cdot 2\text{H}_2\text{O}$ was reacted with $\text{SnCl}_2 \cdot 2\text{H}_2\text{O}$ in triethylene glycol at 205 °C, CZTS nanoplates with the thickness of about 35 nm were obtained.^[9] All these methods start from relatively thermodynamically stable Cu_2SnS_3 and CuS. Residuals of these phases are detrimental to the performance of the solar cells because of their narrower band gap and high conductivity.^[10]

Powder X-ray diffraction (PXRD) and Raman spectroscopy are widely accepted methods for characterizing CZTS and its impurity phases.^[11] PXRD is used to determine the crystal structure of materials but cannot distinguish tetragonal $\text{Cu}_2\text{ZnSnS}_4$ from cubic ZnS and Cu_2SnS_3 due to the similarity of the diffraction patterns from these phases (Figure S1). Contrary, Raman spectroscopy yields distinctly different spectra of these phases and as such is a complementary technique to PXRD (Table S1). X-ray absorption near-edge structure^[12] and neutron diffraction^[13] are also helpful to distinguish these phases but are seldom used due to their scarce availability.

Here, we present the synthesis of $\text{Cu}_x\text{Zn}_y\text{Sn}_{2-0.25x-0.5y}\text{S}_4$ (NS-CZTS) by a cation exchange reaction starting with wide bandgap (3.5 eV) and low conductive cubic ZnS and CuCl_2 and SnCl_4 in triethylene glycol. This new method is compared to a previously published similar cation exchange reaction, in which CuS was used instead of ZnS as a starting material.^[9] It is demonstrated that, using ZnS instead of CuS results in a superior

CZTS product, at the same time permitting control of Zn composition. The composition of NS-CZTS was controlled by the feeding ratio of the reactants enabling zinc rich products. The new cation exchange method is expected to promote the development of highly efficient CZTS devices.

Results and discussion

$\text{Cu}_2\text{ZnSnS}_4$ nanosheets were previously synthesized from narrow band CuS using a cation exchange reaction.^[9] We started with this method in an attempt to synthesize high quality CZTS material to be used in efficient solar cells. Hexagonal CuS with 80 nm average crystallite size was synthesized from CuCl_2 and thiourea via the hydrothermal reaction (Figure S2). The product exhibited a characteristic band at 474 cm^{-1} in Raman spectra (Figure S3). The cation exchange reaction was then carried out at $220\text{ }^\circ\text{C}$ for 96 h in a PTFE reactor as described in the literature^[9]. PXRD revealed that the product contained Cu_2S and $\text{Cu}_2\text{ZnSnS}_4$ or possibly other phases with a similar diffraction pattern as that of $\text{Cu}_2\text{ZnSnS}_4$ (Figure S4). However, its Raman spectrum showed only a weak peak at 338 cm^{-1} often assigned to $\text{Cu}_2\text{ZnSnS}_4$ and a high fluorescent background (Figure S5). The cation exchange reaction was further modified by increasing the reaction temperature from $220\text{ }^\circ\text{C}$ to the boiling point of triethylene glycol ($285\text{ }^\circ\text{C}$) and refluxing the mixture for 22 h. The product was NS-CZTS with the average crystallite size of 52 nm but PXRD also contained two additional peaks at 46.6° and 48.8° that could not be reliably assigned and were assumed to be due to impurities (Figure S6). The product was further soaked in either 2.0 M HCl or 1.0 M NH_3 at room temperature for 30 min followed by thorough water washing in the attempt of removing the impurities. The HCl treatment did not change the

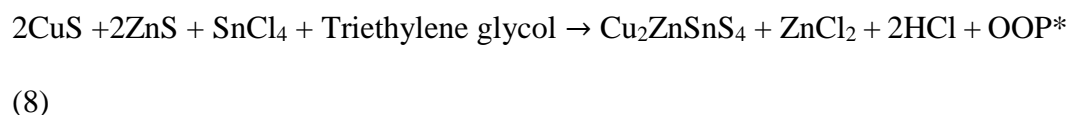
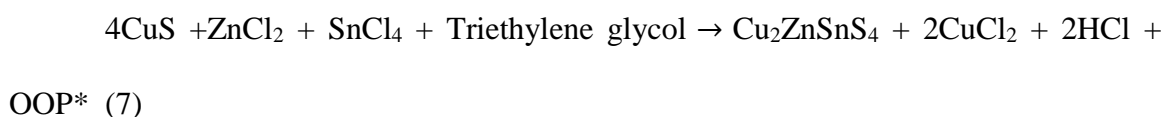
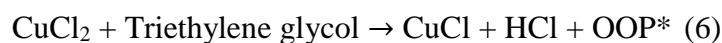
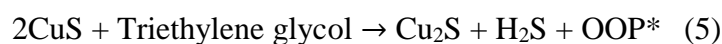
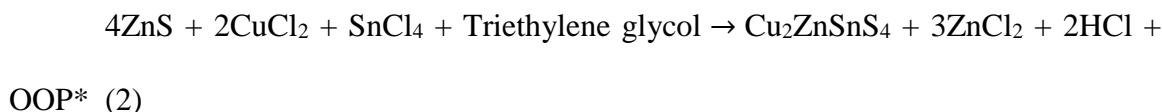
PXRD diffraction pattern of the product as the peaks from the impurities were not removed (Figure S7). In contrast, the impurity peak at 48.8° disappeared after treating with NH_3 .

Raman spectra of the as-synthesized product showed two peaks at 337 and 288 cm^{-1} that are often assigned to non-polar A-symmetry modes of $\text{Cu}_2\text{ZnSnS}_4$.^[14] No observable peak was found around 476 cm^{-1} indicating no detectable Cu_xS in the product (Figure S7). After 30 min treatment with HCl or NH_3 , Raman spectra of the product did not change, but longer reaction times resulted in the formation of Cu_xS as was evident from the appearance of a peak at 476 cm^{-1} . A similar behavior was also observed when using $\text{SnCl}_4 \cdot 5\text{H}_2\text{O}$ instead of SnCl_2 (Figure S4 & S5).

Further studies also showed that this cation exchange reaction was poorly reproducible and the final product was strongly affected by the synthetic history of the CuS. For example, CuS synthesized from 5.0 equivalent thiourea exhibited lower reactivity to Zn^{2+} and Sn^{2+} than that synthesized from 1.0 equivalent thiourea. As a result, the product contained unreacted Cu_2S as was confirmed by the presence of characteristic diffraction peaks at 28.0° (111), 32.4° (200), 46.3° (220), 54.8° (311) in PXRD pattern and a Raman peak at 472 cm^{-1} (Figure S4 & S5). Also, as is shown in the reaction (1), the copper-rich environment promotes the formation the copper-rich product. The copper-rich product is often contained narrow bandgap defects that trap the carriers, thereby reducing the efficiency of photovoltaic devices.^[2] For these reasons, CuS was not considered as a suitable reactant for a cation exchange reaction to produce high quality CZTS.



It was rationalized that if the cation exchange reaction is carried out with ZnS as a starting material, Zn-rich CZTS will result. The following possible reactions were identified.



Note: OOP* = organic oxidation products from triethylene glycol, which are complicated mixtures and will not be discussed here.^[15]

The reaction of ZnS ($pK_{sp} = 26.1$)^[16] with CuCl₂ and SnCl₄ is more thermodynamically favorable than the reaction of CuS ($pK_{sp} = 40.3$)^[16] with Zn(CH₃COO)₂ and SnCl₂ (reaction (2)). The formation of CuS and Cu₂S from ZnS appears also to be thermodynamically feasible and kinetically more favorable than the formation of Cu₂ZnSnS₄ (reactions (3) & (4)) because CuS and Cu₂S have been observed as intermediates (Figure 1–2, S10–S11). CuS can be further reduced to Cu₂S (reaction (5)) and CuCl is produced from CuCl₂ (reaction (6)) by triethylene glycol acting as a reducing agent at high temperature. It is

reasonable to assume that reactions (7), (8), and (9) can proceed because they are similar to reaction (1). According to our results, the reactions (5) proceeded fast when using ZnS with the crystallite size of 5 nm. After adding CuCl₂ into the suspension of 5 nm ZnS in triethylene glycol at room temperature, the white suspension changed to black CuS in 30 seconds. In contrast, ZnS with a crystallite size more than 130 nm reacted significantly slower with CuCl₂ under the same conditions. Specifically, the reaction mixture of ZnS (> 130 nm) and CuCl₂ in triethylene glycol still had white color after stirring at room temperature for 5 h indicating no noticeable CuS. This implies that the formation of CuS is a kinetically controlled reaction that is favorable at low temperatures because $k_B T$ is in the denominator in Arrhenius equation (k_B is the Boltzmann constant and T is the absolute temperature). Therefore, raising the temperature of the cation exchange reaction and using large ZnS crystals favored the formation of CZTS product at the same time minimizing trapping of CuS kinetic product due to increasing rates of reactions (2), (7), (8) and (9).

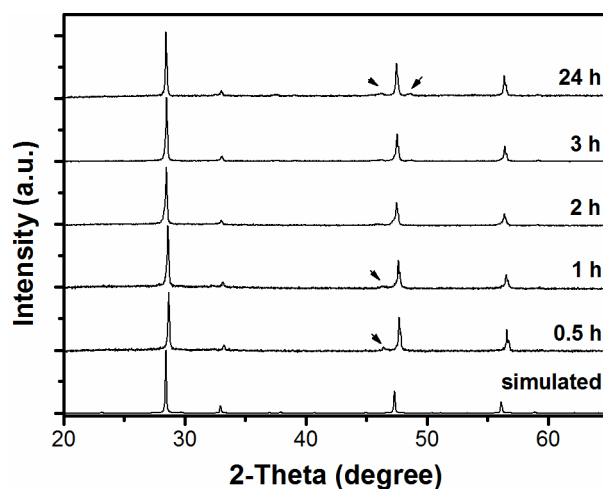


Figure 1. PXRD patterns of NS-CZTS synthesized from ZnS, CuCl₂, and SnCl₄ · 5H₂O at the reflux conditions for different reaction times. The simulated PXRD pattern is of tetragonal Cu₂ZnSnS₄. Diffraction peak at 46.4° is assigned to (220) plane of cubic Cu₂S

(PDF card #: 00-053-0522). Crystallite sizes of NS-CZTS were 123, 112, 101, 120, and 129 nm for the reaction time of 0.5, 1, 2, 3, and 24 h, respectively.

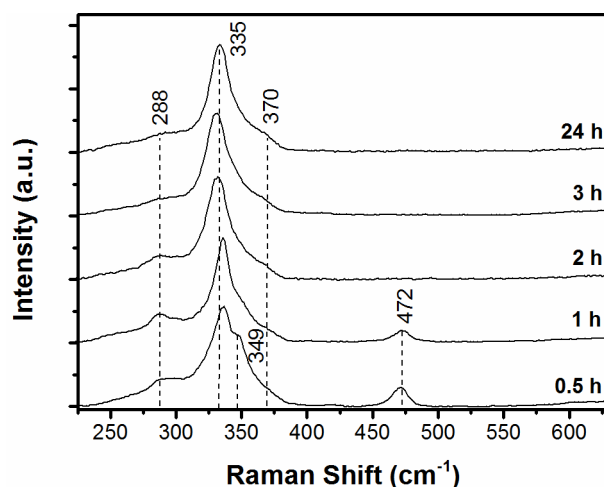


Figure 2. Raman spectra of NS-CZTS synthesized from ZnS, CuCl₂, and SnCl₄ · 5H₂O at the reflux conditions for different reaction times. Raman peaks at 288 and 335 cm⁻¹ are assigned to NS-CZTS; peak at 349 cm⁻¹ is assigned to ZnS, and peak at 472 cm⁻¹ is assigned to Cu₂S.

Highly crystallized ZnS with the crystallite size more than 130 nm was obtained from the hydrothermal reaction of Zn(CH₃COO)₂ with thiourea (Figure S8). The ZnS exhibited a characteristic Raman peak at 351 cm⁻¹ (Figure S9). First, the cation exchange reaction was carried out with tin (II) (SnCl₂), ZnS and CuCl₂ and the product contained NS-CZTS together with unassignable impurities as shown in the PXRD (Figure S10). Only one peak at 337 cm⁻¹ of CZTS was detected in the Raman spectrum (Figure S11). The cation exchange reaction was then carried out using tin (IV) (SnCl₄ · 5H₂O) at 200 °C for 2 h. The product contained a mixture of hexagonal CuS and NS-CZTS as confirmed by PXRD (Figure S10) and Raman showing two peaks at 334 cm⁻¹ from NS-CZTS and at 471 cm⁻¹ from CuS (Figure S11). The reaction temperature was further increased to the boiling

point of triethylene glycol (285 °C). The product contained only NS-CZTS (Figure 1 & 2). The effect of the reaction time on the formation of NS-CZTS was further studied by carrying the reaction at 0.5 h, 1.0 h, 2.0 h, 3.0 h, and 24 h in the mixture of ZnS, CuCl₂, and SnCl₄ · 5H₂O at the reflux reaction condition. Cu₂S was detected as a by-product after the reaction time of 0.5 h and 1.0 h, together with the unreacted ZnS after 0.5 h as indicated by a characteristic Raman peak at 349 cm⁻¹ (Figure 1 & 2). The longest studied reaction time, 24 h, generated also impurities detectable by PXRD but not by Raman spectroscopy. The crystallite size of NS-CZTS did not change when increasing reaction time from 0.5 h to 24 h and was determined by the size of the initial ZnS material because of the nature of cation exchange reactions.

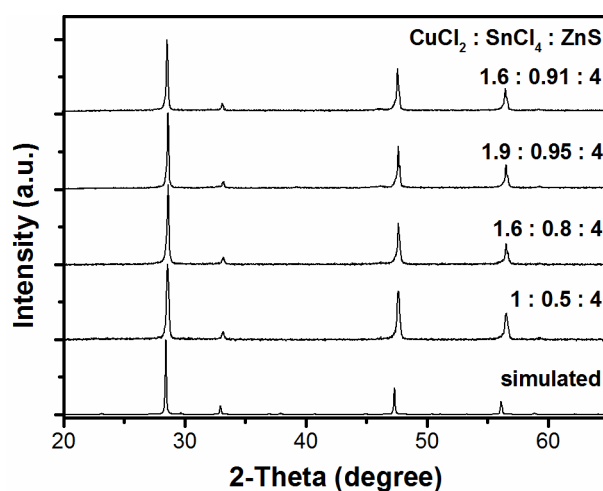


Figure 3. PXRD patterns of NS-CZTS synthesized from ZnS, CuCl₂, and SnCl₄ · 5H₂O with different molar feed ratios at the reflux condition. The simulated PXRD pattern is of tetragonal Cu₂ZnSnS₄. Crystallite sizes of NS-CZTS were 47, 83, 124, and 97 nm for the molar feed ratio of 1 : 0.5 : 4, 1.6 : 0.8 : 4, 1.9 : 0.95 : 4, and 1.6 : 0.91 : 4, respectively.

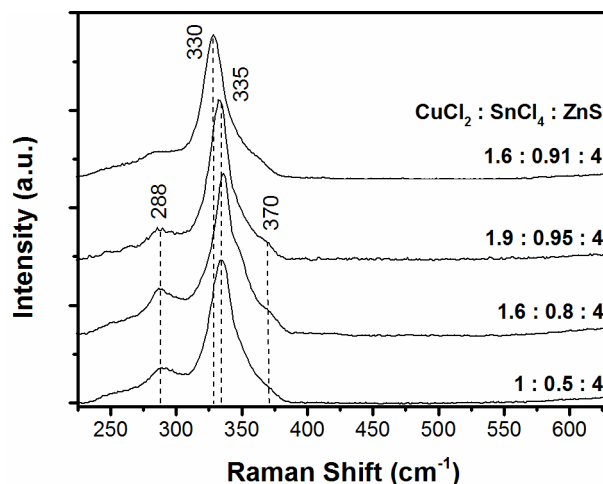


Figure 4. Raman spectra of NS-CZTS synthesized from ZnS, CuCl₂, and SnCl₄ · 5H₂O with different molar feed ratios at the reflux conditions. Raman peaks at 288, 335 and 370 cm⁻¹ are assigned to Cu₂ZnSnS₄.

The effect of the reactant feeding ratios was studied at the reflux condition for 2 h reactions. Only NS-CZTS was formed for the molar feed ratio of CuCl₂ : SnCl₄ : ZnS from 1 : 0.5 : 4 to 1.9 : 0.95 : 4 and the crystallite size increased from 47 nm to 124 nm due to the nonstoichiometric ratio of the reactants (Figure 3 & Table S2). According to literature, the zinc-rich Cu₂ZnSnS₄ with an atom ratio of Cu : Sn : Zn = 1.6 : 0.91 : 1 exhibited high performance in the solar cells. The molar feeding ratio of CuCl₂ : SnCl₄ : ZnS = 1.6 : 0.91 : 4 was also used to synthesize NS-CZTS with a crystallite size of 97 nm. The NS-CZTS material exhibited down shift of the Raman peak from 335 cm⁻¹ to 330 cm⁻¹ when compared to the other materials synthesized from ZnS in this study (Figure 4 & Table S2).

Scanning electron microscopy revealed that ZnS crystallized into the shape of irregular plates and polyhedrons when the reaction was carried out at 220 °C (Figure 5). After the cation exchange reaction with CuCl₂ and SnCl₄ · 5H₂O at the reflux conditions for 2 h, the shape did not change but plates and polyhedrons exhibited rough edges. This

means that the original shape of the ZnS was preserved in the NS-CZTS product.^[6] It was concluded that a desired shape of NS-CZTS can be obtained by controlling the shape of initial ZnS, which is easier to achieve due to the simpler reaction. As such, the described approach provides better control for the preparation of predefined Cu₂ZnSnS₄ nanocrystals.

The synthesized NS-CZTS nanocrystals exhibited a uniform distribution of all elements in any individual particles; however, small particles contained more copper and tin than the large particles, as shown in the EDX elemental maps (Figure 6 & S12–S17). No detectable diffusion edges rich in copper or tin neither ZnS core was found in the elemental maps. Quantitative analysis revealed nonstoichiometric atom ratios that increased from $[Cu]/([Zn] + [Sn]) = 0.12$ & $[Zn]/[Sn] = 31.10$ to $[Cu]/([Zn] + [Sn]) = 0.48$ & $[Zn]/[Sn] = 6.68$ with increasing of the molar feed ratio of CuCl₂ : SnCl₄ : ZnS from 1 : 0.5 : 4 to 1.6 : 0.8 : 4. The further increase of the molar feed ratio to stoichiometric 2 : 1 : 4 yielded the similar atom ratio of $[Cu]/([Zn] + [Sn]) = 0.48$ & $[Zn]/[Sn] = 6.96$. This similarity indicates that the cation exchange of Zn²⁺ by Cu⁺ and Sn⁴⁺ is leveling off while approaching the stoichiometric ratio in the product. The cation exchange reaction should also be controlled by other factors, such as crystal defects in ZnS, which decreased the possibility of the formation of ZnS/NS-CZTS core-shell structure.^[6] The elemental maps of either single large NS-CZTS particle measured using relatively low resolution SEM (Figure S16) or high resolution STEM maps of a single small particle (Figure S17) show no evidence of core-shell structures.

As mentioned in the introduction part, a combination of PXRD and Raman spectroscopy is widely accepted as a standard way for characterizing CZTS materials and their impurities.^[11] It is important to emphasize that the nonstoichiometric NS-CZTS

phases exhibit characteristic PXRD patterns and Raman spectra similar to that of $\text{Cu}_2\text{ZnSnS}_4$ for a broad range of $[\text{Cu}]/([\text{Zn}] + [\text{Sn}])$ of NS-CZTS atom ratios between 0.12 and 0.28. Therefore, it is difficult to distinguish stoichiometric $\text{Cu}_2\text{ZnSnS}_4$ from nonstoichiometric NS-CZTS using the combination of these techniques. The other characterization techniques, such as elemental mapping, are necessary to fully characterize the chemical composition of CZTS materials.

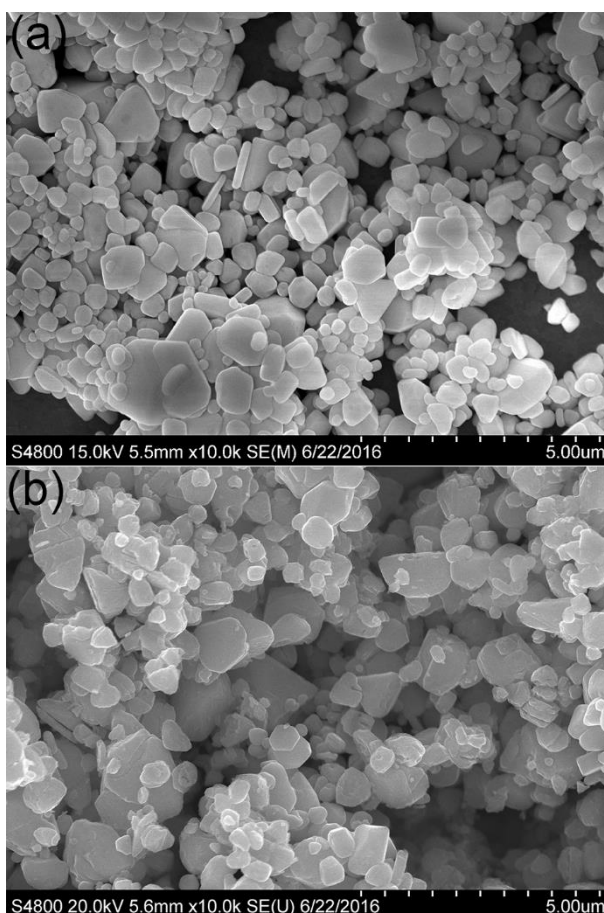


Figure 5. SEM images of (a) ZnS synthesized by the reaction of $\text{Zn}(\text{CH}_3\text{COO})_2$ with thiourea at 220 °C (b) NS-CZTS synthesized from the molar feed ratio of $\text{CuCl}_2 : \text{SnCl}_4 : \text{ZnS} = 2 : 1 : 4$. at reflux condition for 2 h.

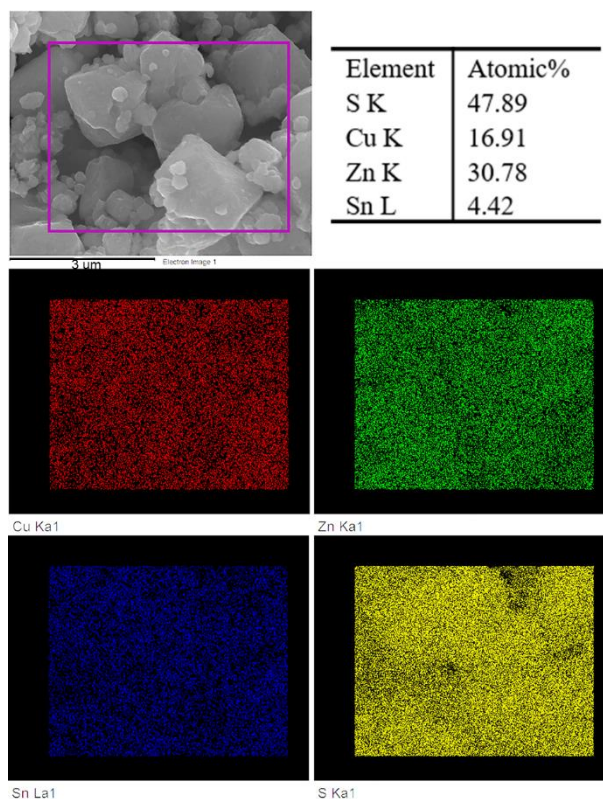


Figure 6. SEM image and EDX elemental maps of NS-CZTS synthesized from the molar feed ratio of $\text{CuCl}_2 : \text{SnCl}_4 : \text{ZnS} = 2 : 1 : 4$, at reflux condition for 2 h.

Conclusion

A new method based on a cation exchange reaction starting with ZnS crystals for the synthesis of nonstoichiometric NS-CZTS with the crystallite size more than 100 nm was developed. The method does not result in the contamination with low bandgap and high conductive Cu_xS impurities that are often detrimental to the applications of CZTS materials. Contrary, the method permits the synthesis of beneficial Zn-rich phases. The synthesized NS-CZTS exhibited a uniform distribution of all elements throughout the individual particles. High similarities of PXRD patterns and Raman spectra of nonstoichiometric NS-CZTS and stoichiometric $\text{Cu}_2\text{ZnSnS}_4$ indicates the importance of using other techniques to fully characterize the chemical composition of the materials. This

cation exchange method is expected to further facilitate the development of $\text{Cu}_2\text{ZnSnS}_4$ based devices.

Experimental section

Materials

Anhydrous tin(II) chloride (Alfa Aesar, 99%), zinc acetate dihydrate (J. T. Baker, Baker analyzed reagent), anhydrous copper (II) chloride, (Acros Organics, 99%), tin (IV) chloride pentahydrate (Fisher Science Education, lab grade), triethylene glycol (TCI, 99.0%) and thiourea (Alfa Aesar, 99%) were used as received.

Instrumentation

Powder X-ray diffraction data was collected using a Rigaku Ultima IV X-ray diffractometer with $\text{Cu K}\alpha$ radiation ($\lambda = 1.5418 \text{ \AA}$) at $25 \text{ }^\circ\text{C}$. PXRD pattern simulation was performed with Mercury 3.5.1 software by using cubic ZnS ($a = 5.40 \text{ \AA}$),^[17] hexagonal CuS ($a = b = 3.729 \text{ \AA}$, $c = 16.11 \text{ \AA}$),^[18] cubic Cu_2SnS_3 ($a = b = c = 5.43 \text{ \AA}$)^[19] and tetragonal $\text{Cu}_2\text{ZnSnS}_4$ ($a = b = 5.434 \text{ \AA}$, $c = 10.850 \text{ \AA}$)^[20] single crystal structures. X-ray powder diffraction analysis was performed on Rigaku PDXL 1.8.1.0 software. Crystallite sizes were calculated from PXRD using Scherrer equation after correcting the instrumental line broadening using the peak width of the width standard data obtained using LaB_6 external standard reference. Electron microscope images were obtained with Hitachi S-4800 field emission scanning electron microscopes (SEM) and HD2000 field emission scanning transmission electron microscope (STEM) equipped with the capability of energy-dispersive X-ray spectroscopy. Particles were drop-casted on polished silicon wafers (Wafer Works Corp., dopant, As, resistivity $\leq 0.006 \text{ } \Omega \cdot \text{cm}$,) for SEM analysis and on copper grids with carbon type-B support films for STEM analysis. Raman spectra were

collected using 514.5 nm excitation light from an Ar⁺ ion laser (Innova 200, Coherent, 500 mW). Scattered light was collected by a f/1.2 camera lens in a backscattering geometry and analyzed by a triple spectrometer (Triplemate 1877, Spex) equipped with a CCD detector (iDUS 420, Andor). Raman spectra of a mixture of chloroform and bromoform were used for the spectral calibration.

Synthesis of CuS

CuCl₂ (0.538 g, 4.00 mmol) was dissolved in hydrochloric acid (4.0 mL, 1.0 mol L⁻¹). Thiourea (0.335 g, 4.4 mmol) was dissolved in H₂O (4.0 mL). The thiourea solution was then added to the CuCl₂ solution drop by drop with stirring at room temperature over a period of 10 min. The reaction mixture was further stirred at room temperature for additional 10 min and then sealed in 23 mL PTFE lined digestion vessel. The reaction mixture was then heated in an oven to a set temperature of 220 °C and kept for 24 h. After cooling to room temperature, the colorless supernatant was discarded and the black precipitate was washed with H₂O three times and then dried in a vacuum oven at 60 °C for 15 h.

Synthesis of NS-CZTS from CuS

Zn(CH₃COO)₂ · 2H₂O (28 mg, 0.13 mmol) and SnCl₂ (25 mg, 0.13 mmol) were dissolved in triethylene glycol (5 mL). CuS (50 mg, 0.52 mmol) was then added to the solution followed by stirring at room temperature for 10 min. The reaction mixture was transferred to 23 mL PTFE lined digestion vessel and kept in an oven at a set temperature of 220 °C for 96 h. Alternatively, the reaction mixture was transferred to a 25 mL round bottom flask and refluxed with stirring for 22 h. After cooling to room temperature, the

reaction mixture was centrifuged and the black precipitate was washed twice with ethanol and twice with water.

Synthesis of ZnS

Zn(CH₃COO)₂ · 2H₂O (2.63 g, 12.0 mmol) and thiourea (0.913 g, 12.0 mmol) were dissolved in H₂O (8 mL). The solution was then transferred to a 23 mL PTFE lined digestion vessel and kept in a 220 °C oven for 24 h. After cooling to room temperature, the colorless supernatant was discarded and the white precipitate was washed with H₂O three times and then dried in a vacuum oven at 60 °C for 15 h.

Synthesis of NS-CZTS from ZnS

CuCl₂ (54 mg, 0.40 mmol) and SnCl₄ · 5H₂O (70 mg, 0.20 mmol) were dissolved in triethylene glycol (5 mL). ZnS (78 mg, 0.80 mmol) was then added to the solution followed by refluxing for 3 h. After cooling to room temperature, the reaction mixture was centrifuged and separated into a slightly yellow-brown supernatant and a black precipitate. The black precipitate was washed twice with ethanol and twice with water.

Supporting information

Supporting information and ORCID(s) from the author(s) for this article are available on the WWW under <http://dx.doi.org/> .

Acknowledgments

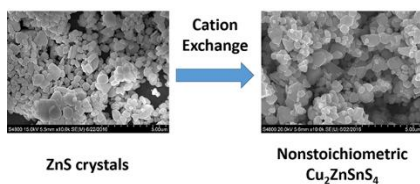
We gratefully acknowledge the support of this work from Clemson University Center for Optical Materials Science and Engineering Technologies.

References

- [1] J. Wang, N. Yu, Y. Zhang, Y. Zhu, L. Fu, P. Zhang, L. Gao, Y. Wu, *J. Alloys Compd.* **2016**, 688, 923-932.
[2] a) C. Yan, F. Liu, K. Sun, N. Song, J. A. Stride, F. Zhou, X. Hao, M. Green, *Sol. Energy Mater. Sol. Cells* **2016**, 144, 700-706; b) D. Nam, S. Cho, J.-H. Sim, K.-J. Yang,

- D.-H. Son, D.-H. Kim, J.-K. Kang, M.-S. Kwon, C.-W. Jeon, H. Cheong, *Sol. Energy Mater. Sol. Cells* **2016**, *149*, 226-231.
- [3] Y. Yang, W. Que, X. Zhang, X. Yin, Y. Xing, M. Que, H. Zhao, Y. Du, *Appl. Catal., B* **2017**, *200*, 402-411.
- [4] X. Yu, J. Liu, A. Genç, M. Ibáñez, Z. Luo, A. Shavel, J. Arbiol, G. Zhang, Y. Zhang, A. Cabot, *Langmuir* **2015**, *31*, 10555-10561.
- [5] M.-J. Zhang, Q. Lin, X. Yang, Z. Mei, J. Liang, Y. Lin, F. Pan, *Nano Lett.* **2016**, *16*, 1218-1223.
- [6] L. De Trizio, L. Manna, *Chem. Rev.* **2016**, *116*, 10852-10887.
- [7] Y.-X. Wang, M. Wei, F.-J. Fan, T.-T. Zhuang, L. Wu, S.-H. Yu, C.-F. Zhu, *Chem. Mater.* **2014**, *26*, 5492-5498.
- [8] X.-J. Wu, X. Huang, X. Qi, H. Li, B. Li, H. Zhang, *Angew. Chem., Int. Ed.* **2014**, *53*, 8929-8933.
- [9] B.-J. Li, P.-F. Yin, Y.-Z. Zhou, Z.-M. Gao, T. Ling, X.-W. Du, *RSC Adv.* **2015**, *5*, 2543-2549.
- [10] a) S. Siebentritt, S. Schorr, *Prog. Photovoltaics* **2012**, *20*, 512-519; b) J. Tao, J. Liu, L. Chen, H. Cao, X. Meng, Y. Zhang, C. Zhang, L. Sun, P. Yang, J. Chu, *Green Chem.* **2016**, *18*, 550-557.
- [11] G. Altamura, J. Vidal, *Chem. Mater.* **2016**, *28*, 3540-3563.
- [12] J. Just, D. Luetzenkirchen-Hecht, R. Frahm, S. Schorr, T. Unold, *Appl. Phys. Lett.* **2011**, *99*, 262105.
- [13] S. Schorr, *Sol. Energy Mater. Sol. Cells* **2011**, *95*, 1482-1488.
- [14] M. Guc, S. Levchenko, I. V. Bodnar, V. Izquierdo-Roca, X. Fontane, L. V. Volkova, E. Arushanov, A. Pérez-Rodríguez, *Sci. Rep.* **2016**, *6*, 19414.
- [15] A. Satta, D. Shamiryan, M. I. R. Baklanov, C. M. Whelan, Q. Toan Le, G. P. Beyer, A. Vantomme, K. Maex, *J. Electrochem. Soc.* **2003**, *150*, G300-G306.
- [16] S. Licht, *J. Electrochem. Soc.* **1988**, *135*, 2971-2975.
- [17] I. Khan, I. Ahmad, H. A. Rahnamaye Aliabad, M. Maqbool, *J. Appl. Phys.* **2012**, *112*, 073104.
- [18] Y. Takeuchi, Y. Kudoh, G. Sato, *Z. Kristallogr.* **1985**, *173*, 119-128.
- [19] L. S. Palatnik, Y. F. Komnik, V. M. Koshkin, E. K. Belova, *Dokl. Akad. Nauk SSSR* **1961**, *137*, 68-71.
- [20] L. Choubrac, A. Lafond, C. Guillot-Deudon, Y. Moëlo, S. Jobic, *Inorg. Chem.* **2012**, *51*, 3346-3348.

Table-of-Contents



A cation exchange reaction of ZnS with CuCl_2 and SnCl_4 was developed to synthesize nonstoichiometric $\text{Cu}_2\text{ZnSnS}_4$ with crystallite size more than 100 nm. The method allows the formation of Zn-rich phases and good control of the crystal size and shape.